Published in final edited form as:
Exp Parasitol. 2012 June ; 131(2): 245–251. doi:10.1016/j.exppara.2012.03.005.

Modifications in Erythrocyte Membrane Zeta Potential by *Plasmodium falciparum* Infection

Fuyuki Tokumasu[a,*], **Graciela R. Ostera**[b], **Chanaki Amaratunga**[a], and **Rick M. Fairhurst**[a]

[a]Laboratory of Malaria and Vector Research, National Institute of Allergy and Infectious Diseases, National Institutes of Health, Bethesda, MD, 20892-8132, USA

[b]Department of Biochemistry and Molecular Biology, Georgetown Medical Center, Washington DC, 20007, USA

Abstract

The zeta potential (ZP) is an electrochemical property of cell surfaces that is determined by the net electrical charge of molecules exposed at the surface of cell membranes. Membrane proteins contribute to the total net electrical charge of cell surfaces and can alter ZP through variation in their copy number and changes in their intermolecular interactions. *Plasmodium falciparum* extensively remodels its host red blood cell (RBC) membrane by placing 'knob'-like structures at the cell surface. Using an electrophoretic mobility assay, we found that the mean ZP of human RBCs was −15.7 mV. In RBCs infected with *P. falciparum* trophozoites ('iRBCs'), the mean ZP was significantly lower (−14.6 mV, $p<0.001$). Removal of sialic acid from the cell surface by neuraminidase treatment significantly decreased the ZP of both RBCs (−6.06 mV) and iRBCs (−4.64 mV). Parasite-induced changes in ZP varied by *P. falciparum* clone and the presence of knobs on the iRBC surface. Variations in ZP values were accompanied by altered binding of iRBCs to human microvascular endothelial cells (MVECs). These data suggest that parasite-derived knob proteins contribute to the ZP of iRBCs, and that electrostatic and hydrophobic interactions between iRBC and MVEC membranes are involved in cytoadherence.

Keywords

zeta potential; *Plasmodium falciparum*; knob; cytoadherence; erythrocyte membrane

1. Introduction

Plasmodium falciparum causes the most deadly form of human malaria. During its stage of intraerythrocytic development, the parasite dramatically remodels the membrane of its host red blood cell (RBC) (Haldar and Mohandas, 2007, Maier, et al., 2009, Murphy, et al., 2007). The most significant morphological membrane modification in *P. falciparum* trophozoite-infected RBCs ('iRBCs') is the placement of electron-dense 'knobs' that protrude from the iRBC surface (Aikawa, et al., 1996, Nagao, et al., 2000). Knobs are complex structures formed by the aggregation of RBC- and parasite-derived proteins (Cooke, et al., 2000). Several parasite-derived proteins, including *P. falciparum* erythrocyte

*Corresponding Author: Fuyuki Tokumasu, Ph.D., 12735 Twinbrook Parkway, Room 2W09B, Bethesda, MD 20892-8132, Phone: 301-451-1224, Fax: 301-480-1438, ftokumasu@niaid.nih.gov.

membrane protein 1 (PfEMP1) and knob-associated histidine rich protein (KAHRP), traffic to the iRBC membrane where they are incorporated into knobs. These knobs provide a platform for the display of PfEMP1, the parasite's main cytoadherence ligand and virulence factor, which mediates binding of iRBCs to various receptors (e.g., CD36, ICAM-1) on human microvascular endothelial cells (MVECs) (Baruch, et al., 1997, Buffet, et al., 1999, Chen, et al., 2000). Numerous other parasite-derived proteins, which are known to be expressed at the iRBC surface or were found to contain host-targeting sequence signals, also take part in the complex membrane remodeling process that accompanies *P. falciparum* development (Haldar, et al., 2006, Maier, et al., 2009). We hypothesized that these modifications could significantly impact the electrochemical dynamics of the iRBC surface and the physical interaction of iRBCs with other cells. A detailed study of how *P. falciparum* infection changes the RBC membrane surface potential at the cellular level has not been reported.

The zeta potential (ZP), an electrochemical property of cell surfaces, is determined by the net electrical charge of surface-exposed molecules. The RBC membrane is negatively charged and is surrounded by a fixed layer of cations in the medium (Fig. 1). This fixed layer of cations is surrounded by a cloud-like diffused layer of a mixture of cations and anions. Within the diffused layer, Brownian motion of RBCs and the flow of medium creates a 'shear' plane, which separates unfixed ions from those ions closely associated with the fixed layer. The potential at the shear plane is defined as the ZP. To improve our understanding of cytoadherence phenomena, we analyzed the impact of *P. falciparum* infection on the ZP of RBCs, and investigated the effects of knob and other iRBC surface modifications on the adherence of iRBCs to MVECs.

2. Materials and Methods

2.1 Parasite cultivation

P. falciparum clones 3D7, Indochina and 3D7 KAHRP knockout ('KAHRP(−) 3D7') (Malaria Research and Reference Reagent Resource Center, Manassas, VA) were cultured in O+ RBCs (Interstate Blood Bank, Memphis, TN) at 5% hematocrit in RPMI-1640 media supplemented with 25 mg/ml HEPES, 2 mg/ml sodium bicarbonate, 50 μg/ml gentamicin and 0.5% Albumax II (Invitrogen, Carlsbad, CA). In all comparisons between RBCs and parasitized RBCs, RBCs from the same donor were mock-cultured alongside parasitized RBC samples. Parasites were synchronized weekly at the trophozoite stage by Percoll-sorbitol gradient centrifugation.

2.2 Zeta potential measurements

RBCs and parasitized RBCs were resuspended in HEPES buffer, pH 7.05, at 0.1% hematocrit and transferred into a Zeecom Zeta Potential Analyzer (Mircrotec, Chiba, Japan) (Tokumasu, et al., 2009). Prior to data collection, pH and temperature in these RBC suspensions were measured and detection parameters for ZP measurements such as light intensity, focal plane and tracking duration were optimized for stable data collection. The RBC suspensions were then subjected to electrophoresis at 20 V. The mobility of individual RBCs was tracked by equipped Zeecom software using microscopically-acquired video images, and data were collected using a standard Helmholtz-Smoluchowski formula (Overbeek, 1952, Weiss and Woodbridge, 1967). The dielectric constant of HEPES buffer was approximated as that of water; the deviation of the dielectric constant was negligible, ≈2% (Hasted, et al., 1948). Statistical analyses including t-test and Gaussian curve fitting of the data were performed with Origin 8.0 software (OriginLab, Northampton, MA).

2.3 Neuraminidase treatment to remove sialic acid from the RBC surface

Sialic acid, a major contributor to RBC surface potential, was removed by neuraminidase treatment to study the net charge from membrane proteins and lipids. RBCs and iRBCs at 0.1% hematocrit were incubated with 2.5 units of neuraminidase from *Clostridium perfringens* (Sigma, St. Louis, MO) in HEPES buffer containing Complete® protease inhibitor (Roche, Mannheim, Germany) for 1 h at 37°C with periodic agitation. RBCs were washed and resuspended in 8 ml HEPES buffer before ZP measurements.

2.4 Trypsin treatment to remove trypsin-sensitive proteins from the RBC surface

To structurally modify proteins on RBC surface, including PfEMP1 proteins that mediate cytoadherence, RBCs were treated with 10 μg/ml trypsin in HEPES for 30 min at room temperature. Cells were washed with HEPES buffer twice and resuspended in 8 ml HEPES buffer before ZP measurements.

2.5 Scanning and transmission electron microscopy

iRBCs were purified to >80% parasitemia from cultures using a MACS® magnetic separation column (Miltenyi Biotec, Auburn, CA). To image these iRBCs by scanning electron microscopy (SEM), approximately 30 μl of purified parasite suspension in RPMI-1640 media was directly applied to silicon chips (Ted Pella, Inc., Redding, CA) and incubated for 10–15 min. Excess media was absorbed by filter paper and iRBCs were fixed by a method modified to retain RBC structure (Tokumasu and Dvorak, 2003). In brief, iRBC membranes were crosslinked with dimethylsuberimidate (DMS) (Sigma) in 100 mM sodium borate buffer, pH 9.5, containing 1 mM $MgCl_2$ for 1 h, then fixed with 2.5% glutaraldehyde/4.0% paraformaldehyde in 0.1 M sodium cacodylate buffer pH 7.4 (Electron Microscopy Sciences, Hatfield, PA) for 15 min, and then quenched with 0.1 M glycine in PBS, pH 7.4, for 1 h. For transmission electron microscopy (TEM), iRBCs were fixed in the same manner but in suspension.

Following fixation, the chips were washed twice in cacodylate buffer and post-fixed with 1% osmium tetroxide (Ted Pella, Inc.) in cacodylate (OTO) for 30 min. After three washes with water, the samples were treated with saturated thiocarbohydrazide (Electron Microscopy Sciences) in water for 30 min, washed three times in water, and re-treated with OTO for 30 min. Following three washes in water, the samples were dehydrated in ethanol and critical point-dried through carbon dioxide using a Model CPD-030 critical point drier (Bal-Tec, Brookline, NH). The chips were then mounted onto stubs, lightly sputtered with chromium (Refining Systems, Inc., Las Vegas, NV) by a Model IBS/e ion beam sputterer (South Bay Technologies, San Clemente, CA), and examined at 2 kV with a Model S5200 in-lens field emission scanning electron microscope equipped for digital imaging (Hitachi High Technologies, Pleasanton, CA).

For TEM, fixed iRBC pellets were gently resuspended in approximately 40 μL of 2% NuSieve low-melt agarose (Cambrex, East Rutherford, NJ) in 0.1 M cacodylate buffer, pH 7.2, and chilled until solidified. Small 1–2 mm cubes of agarose containing iRBCs were excised and processed as follows. After washing in cacodylate buffer for 30 min, the samples were post-fixed in 1% osmium tetroxide/0.8% potassium ferrocyanide in cacodylate buffer for 2 h. Samples were washed once in cacodylate buffer and twice in water, and then stained in-block with 1% uranyl acetate for 1 h. After two washes with water, samples were dehydrated in acetone and embedded in araldite resin (Electron Microscopy Sciences). Thin sections were cut with a diamond knife (Diatome 35° knife) and examined at 80 kV with a model H7500 transmission electron microscope (Hitachi High Technologies). Images were captured with an XR-100 CCD camera system (Advanced Microscopy Technologies, Danvers, MA).

2.6 Cytoadherence Assays

Cytoadherence assays were carried out as previously described (Cholera, et al., 2008). Briefly, iRBCs were purified by magnetic columns (>95% parasitemia) and adjusted to 20% parasitemia and 1% hematocrit by adding RBCs in binding media (BM: RPMI-1640, 0.5% BSA, pH 6.7). Human dermal MVECs (Lonza, Walkersville, MD) were cultured in the manufacturer's EGM-2MV medium and grown on LabTek CC2-coated 8-well chamber slides (Nalge Nunc International, Naperville, IL). Prior to the assay, the EGM-2MV medium was removed from the chamber slide and 150 μL BM was added to each well, followed by 150 μL iRBC suspension (in duplicate for each *P. falciparum* clone or neuraminidase/trypsin treated sample), and incubated at 37°C for 1 h with orbital agitation. iRBC suspensions were removed, and adherent MVECs were washed by dipping the slide four times in BM, fixed in 2% gluteraldehyde at ambient temperature overnight, and stained with 10% Giemsa for 30 min. The number of iRBCs bound to approximately 700 MVECs was counted from duplicate wells. For each slide the number of *P. falciparum* Indochina-iRBCs or KAHRP(−) 3D7-iRBCs were normalized to counts from 3D7-iRBCs. Similarly, results from neuraminidase- and trypsin-treated iRBCs were normalized to those from untreated iRBCs for each *P. falciparum* clone.

3. Results

The ZP values of RBC membrane surfaces was measured using an electrophoretic mobility device monitored by a microscopic tracking system described by Jan and Chien (Jan and Chien, 1973). To investigate whether RBC membrane remodeling by *P. falciparum* influences cell surface charge, we compared ZP values between RBCs and parasitized RBCs. To control for the possibility that *in vitro* culture conditions generate biochemical changes in RBCs (e.g., hemoglobin auto-oxidation, binding of hemichromes to the inner leaflet of the RBC membrane, and adsorption of soluble proteins from the culture medium) that modify ZP, we mock-cultured RBCs alongside parasitized RBCs. Since biochemical variations between donor RBC samples, such as the age-distribution of RBCs, may influence ZP values, mock-cultured RBCs from the same donor provides the best baseline ZP measurement for each sample. We found that the mean ZP of ring-infected RBCs did not significantly differ from that of RBCs (−15.2 mV *vs.* −15.0 mV, p=0.93) (Table; Fig. 2A), although the position of the ZP peak and the width of the ZP distribution differed slightly between RBC samples. However, we did find that the mean ZP of iRBCs was significantly lower than that of RBCs (−14.6 mV *vs.* −15.7 mV, p<0.001) (Table; Fig. 2B). This difference was due to the increased number of RBCs with lower ZP at ≈ 13 mV as well as the decreased number of RBCs with higher ZP at >15 mV. Although a decrease in absolute ZP implies a smaller intercellular repulsive force, we observed negligible self-aggregation of iRBCs in the ZP measuring device.

A major contributor to the negative ZP of RBCs is sialic acid, which is abundantly present on the RBC surface (Eylar, et al., 1962, Jan and Chien, 1973). This negative charge on the RBC surface is believed to prevent RBC aggregation, as removal of sialic acid residues by neuraminidase treatment causes RBC aggregation (Jan and Chien, 1973). To measure the contribution of sialic acid to the ZP of RBCs and iRBCs, we treated these cells with neuraminidase. After neuraminidase treatment, we found that the ZP of treated RBCs and iRBCs was, as expected, significantly lower than that of untreated RBCs and iRBCs (p<0.001) (Table; Figs. 2B and 2C). The ZP values of neuraminidase-treated iRBCs were more widely distributed, but the peak ZP value remained significantly lower than that of neuraminidase-treated RBCs (−4.64 mV *vs.* −6.06 mV, p<0.001) (Table; Fig. 2C). These observations suggest that parasite-induced modifications in the RBC membrane alter its electrochemical properties in a manner that is independent of sialic acid. The expression of parasite-derived proteins or parasite-induced changes in RBC protein distribution (as occurs

with knob formation) may have increased the dispersion of ZP values between neuraminidase-treated iRBCs and RBCs.

To investigate the relationship between ZP and the presence of knobs on iRBCs, we compared the ZP values of knobby 3D7-iRBCs and knobless Indochina-iRBCs (Ardeshir et al., 1987). We also measured the ZP of KAHRP(−) 3D7-iRBCs that do not express the knob-forming KAHRP protein due to genetic disruption of the parasite *kahrp* gene (Crabb, et al., 1997). SEM and TEM images confirmed that 3D7-iRBCs (Fig. 3A, **panels b and f**) displayed knobs, and that Indochina-iRBCs (Fig. 3A, **panels c and g**) and KAHRP(−) 3D7-iRBCs (Fig. 3A, **panels d and h**) lacked knobs. No other RBC membrane modifications were observed in knobless Indochina- or KAHRP(−) 3D7-iRBCs.

We found that knobless Indochina-iRBCs showed greater variability in ZP values than knobby 3D7-iRBCs (−14.4 ± 2.7 mV (Indochina) *vs.* −14.8 ± 1.7 mV (3D7)) (mean ± sd, p=0.04) (Fig. 3B). This was probably due to the increased number of Indochina-iRBCs with relatively low ZP values (≈−13 mV). The mean ZP of the entire population of Indochina-iRBCs was approximately 1.6 mV lower than the mean ZP of mock-cultured RBCs (−14.4 mV *vs.* −16.0 mV, p<0.0001) (Fig. 3B). This difference is 0.5 mV greater than the difference between 3D7-iRBCs and mock-cultured RBCs (−14.6 mV *vs.* −15.7 mV) (Fig. 2B; Table). In contrast, the mean ZP of KAHRP(−) 3D7-iRBCs did not differ significantly from that of mock-cultured RBCs (−15.4 mV *vs.* −15.4 mV, p=0.89) (Fig. 3C). These data show that 3D7-, Indochina- and KAHRP(−) 3D7-iRBCs have different compositions of charged molecules on their surface.

To investigate possible relationships between the charged molecule profile of iRBC surfaces and cytoadherence interactions, we compared the binding of 3D7-, Indochina- and KAHRP(−) 3D7-iRBCs to human dermal microvascular endothelial cells (MVECs) expressing the major host cytoadherence receptor CD36 under semi-static conditions. We counted the number of iRBCs bound to ≈700 MVECs and expressed the data as a ratio of the number of iRBCs per MVEC. For 3D7, we found a mean ratio of 1.2 iRBCs bound per MVEC (Fig. 3D) and defined this ratio as 100% binding. iRBCs containing knobless Indochina parasites – which lack knobs and most surface PfEMP1 proteins – did not bind MVECs significantly under the conditions of our assay (Fig. 3D). For KAHRP(−) 3D7, we also found no reduction in the binding of iRBCs to MVECs, although the binding ratios were more variable (Fig. 3D). This finding suggests that the binding was destabilized in KAHRP(−) 3D7 parasites, or that the cell surface configuration of PfEMP1 was not optimal. These results are similar to those of Horrocks *et al.* (Horrocks, et al., 2005) and Crabb *et al.* (Crabb, et al., 1997) who reported differences in cytoadherence between isogenic knobby and knobless *P. falciparum* clones.

Decreases in ZP values of iRBC and neuraminidase-treated RBCs and iRBCs suggest a decrease in electrostatic repulsion forces between cells and a relative increase in hydrophobic and local Van der Waals forces between cells in close proximity. These predictions are supported by the >60% increase in cytoadherence of neuraminidase-treated 3D7-iRBCs compared to untreated 3D7-iRBCs (100% vs. 166.8%, p=0.003) (Fig. 3E). The major cytoadherence ligand PfEMP1 is sensitive to trypsin cleavage from the surface of iRBCs. As expected, trypsin treatment of iRBCs abolished cytoadherence to less than 1%, suggesting that cytoadherence is predominantly mediated by PfEMP1 and perhaps other trypsin-sensitive proteins exposed on the iRBC surface. While Indochina-iRBCs showed almost no cytoaherence to MVECs (Fig. 3D), neuraminidase treatment of these cells increased their adherence (100% *vs.* 135%, p=0.43), although this difference was not statistically significant. Neuraminidase – treatment also increased the adherence of KAHRP(−) 3D7-iRBCs to MVECs (100% *vs.* 111%, p=0.21), but this difference was also

not statistically significant. Data from all three *P. falciparum* clones suggest that the optimal level of negative charge on the iRBC surface could help stabilize specific cell-cell interactions.

4. Discussion

Zeta potential is determined by surface net charge of RBCs along with chemical conditions in surrounding media. Factors that impact surface ZP values in each sample also include the age-distribution of RBCs and intrinsic donor-related variations in RBC surfaces. Aging of RBCs is known to induce surface modifications of membrane proteins and lipids that are similar to those observed in iRBCs, as discussed below. Further analyses indicate that aged RBCs in density-fractionated blood samples had lower ZP than young RBCs (data not shown), suggesting that unequal age-distributions in populations of RBCs between samples could affect ZP estimates. In fact, we occasionally noticed small changes in the width of ZP distributions and the height of ZP peaks between samples. To minimize estimation errors due to sample variation, we studied mock-cultured RBCs in all experiments. In the technical aspect of our work, careful adjustment of measurement parameters was required for the accuracy of electrophoresis-based ZP measurements. For example, the flow speeds of liquid and cells change as a function of the distance from the chamber wall. Adjustment of focal depth was thus important to obtain consistent data. Electrolysis-induced pH changes also affect the size of electric double layer (fixed layer and diffused layer up to the shear plane, Fig. 1) surrounding RBCs. The prolonged measurement also causes bubbles from electrodes that changes the flow rate, flow pattern, and efficiency of electrolysis. All of these factors will result in measurement errors.

One major finding of this study was that *P. falciparum* induces changes in the ZP of RBCs. While we have not determined how parasites alter the net surface charge of RBCs, several possibilities exist. *P. falciparum* inserts numerous proteins in its host cell membrane that, along with RBC membrane proteins, form knobs and other protein clusters at the iRBC surface (Fairhurst, et al., 2005, Nagao, et al., 2000). Parasite infection also induces clustering or remodeling of RBC membrane proteins (Tokumasu, et al., 2005, Tokumasu, et al., 2009). Examples of this phenomenon are the clustering of band 3, a Cl/HCO_3^- exchanger present in $\approx 1\times10^6$ copies per RBC membrane, and the degradation of band 3 by parasite proteases (Giribaldi, et al., 2001, Roggwiller, et al., 1996, Tokumasu, et al., 2005). As a result of these dynamic changes, electrostatic interactions between adjacent molecules may cancel out some surface charges or induce lateral protein-protein interactions that alter protein distributions. Parasite infection of RBCs also induces the partial uptake of proteins into detergent-resistant membrane (DRM) microdomains (‘rafts’) (Murphy, et al., 2004, Nagao, et al., 2002), which changes the overall composition of the RBC membrane. It was reported that two key constituents of DRMs, cholesterol and sphingomyelin, significantly decrease during parasite infection of RBCs (Maguire and Sherman, 1990). Exposure of negatively-charged phosphatidylserine has also been observed during *P. falciparum* infection (Eda and Sherman, 2002). These marked alterations in lipid composition and protein expression may facilitate changes in the lateral distribution of lipid-protein complexes and membrane phase behaviors (London, 2005), both of which could affect the ZP of RBCs (Tokumasu, et al., 2009).

Interestingly, we observed that knobless Indochina-iRBCs showed lower negative ZP than knobless KAHRP(−) 3D7-iRBCs. In the Indochina parasite line, *kahrp* is deleted along with 18 additional genes in the subtelomeric region of chromosome 2 (Gardner, et al., 2002). Some of these proteins are predicted to traffic to the iRBC surface and may account for differences in ZP between Indochina-iRBCs and KAHRP(−) 3D7-iRBCs, in which only the *kahrp* gene has been disrupted (Crabb, et al., 1997). We also observed differences in ZP

distributions between iRBCs containing isogenic knobby 3D7 and knobless KARHP(−) 3D7 parasites, although the mean ZP values were identical. These differences may be due to lateral rearrangements of both RBC- and parasite-derived proteins involved in knob formation, a process that can be expected to modulate the net surface charge in 3D7-iRBCs. The ZP values obtained from knobless KAHRP(−) 3D7-iRBCs suggest, however, that iRBCs may experience this lateral rearrangement in the absence of KAHRP.

Our cytoadherence data suggest that removing negative surface charge by neuraminidase treatment increases the adherence of both knobby and knobless iRBCs to MVECs. Presumably, the removal of sialic acid reduces intercellular repulsive forces, thereby increasing the net attractive force between iRBCs and MVECs. In constrast, repulsive forces between membranes may help increase the specificity of more dominant binding factors such as PfEMP1. Increasing cytoadherence by neuraminidase treatment may suggest that both non-specific interactions and weak non-PfEMP1 protein-protein interactions exist. This hypothesis was partially supported by a modest increase in the cytoadherence of Indochina and KAHRP(−) 3D7 iRBCs, suggesting that weak but specific trypsin-sensitive interactions exist. Although it is generally accepted that PfEMP1-mediated interactions are the dominant factors involved in cytoadherence, our ZP data suggest that weaker, non-PfEMP1 protein-protein interactions may also be involved in cytoadherence, probably originating from other parasitic proteins also inserted in the iRBC membrane. In addition to classical electrostatic interactions, a variety of long- and short-range intercellular forces (e.g., membrane fractuations) and ionic dispersion forces (Bostrom, et al., 2001), may also be altered by *P. falciparum* in ways that promote or stabilize cell-cell interactions. In conclusion, membrane protein interactions between cells are (biophysically or mechanically) very small-scale reactions within adjacent large matrices (i.e., cell membrane), suggesting that other molecular interactions in membranes should be considered. Our data suggest that the specificity of certain protein-protein interactions are due to the net differences between specific and non-specific interactions. In this context, each specific protein-protein interaction is determined by the relative balance between intermolecular binding and repulsive forces.

Acknowledgments

This research was supported by the Intramural Research Program of the NIAID, NIH. We thank Drs. Thomas E. Wellems, NIAID/NIH, and Eri Hayakawa, Jichi Medical University, Japan, for critical reviews of the manuscript and helpful discussions. We also thank Dr. David Dorward, NIAID/NIH, for technical help with electron microscope imaging.

References

Aikawa M, Kamanura K, Shiraishi S, Matsumoto Y, Arwati H, Torii M, Ito Y, Takeuchi T, Tandler B. Membrane knobs of unfixed Plasmodium falciparum infected erythrocytes: new findings as revealed by atomic force microscopy and surface potential spectroscopy. Exp Parasitol. 1996; 84:339–343. [PubMed: 8948323]

Ardeshir F, Flint TJ, Matsumoto Y, Aikawa M, Reese RT, Stanley H. cDNA sequence encoding a Plasmodium falciparum protein associated with knobs and localization of the protein to electron dense regions in membranes of infected erythrocytes. EMBO J. 1987; 6:1421–1427. [PubMed: 3301326]

Baruch DI, Ma XC, Singh HB, Bi X, Pasloske BL, Howard RJ. Identification of a region of PfEMP1 that mediates adherence of Plasmodium falciparum infected erythrocytes to CD36: conserved function with variant sequence. Blood. 1997; 90:3766–3775. [PubMed: 9345064]

Bostrom M, Williams DR, Ninham BW. Specific ion effects: why DLVO theory fails for biology and colloid systems. Phys Rev Lett. 2001; 87:168103. [PubMed: 11690249]

Buffet PA, Gamain B, Scheidig C, Baruch D, Smith JD, Hernandez-Rivas R, Pouvelle B, Oishi S, Fujii N, Fusai T, Parzy D, Miller LH, Gysin J, Scherf A. Plasmodium falciparum domain mediating adhesion to chondroitin sulfate A: a receptor for human placental infection. Proc Natl Acad Sci U S A. 1999; 96:12743–12748. [PubMed: 10535993]

Chen Q, Heddini A, Barragan A, Fernandez V, Pearce SF, Wahlgren M. The semiconserved head structure of Plasmodium falciparum erythrocyte membrane protein 1 mediates binding to multiple independent host receptors. J Exp Med. 2000; 192:1–10. [PubMed: 10880521]

Cholera R, Brittain NJ, Gillrie MR, Lopera-Mesa TM, Diakite SA, Arie T, Krause MA, Guindo A, Tubman A, Fujioka H, Diallo DA, Doumbo OK, Ho M, Wellems TE, Fairhurst RM. Impaired cytoadherence of Plasmodium falciparum-infected erythrocytes containing sickle hemoglobin. Proc Natl Acad Sci U S A. 2008; 105:991–996. [PubMed: 18192399]

Cooke B, Coppel R, Wahlgren M. Falciparum malaria: sticking up, standing out and outstanding. Parasitol Today. 2000; 16:416–420. [PubMed: 11006472]

Crabb BS, Cooke BM, Reeder JC, Waller RF, Caruana SR, Davern KM, Wickham ME, Brown GV, Coppel RL, Cowman AF. Targeted gene disruption shows that knobs enable malaria-infected red cells to cytoadhere under physiological shear stress. Cell. 1997; 89:287–296. [PubMed: 9108483]

Eda S, Sherman IW. Cytoadherence of malaria-infected red blood cells involves exposure of phosphatidylserine. Cell Physiol Biochem. 2002; 12:373–384. [PubMed: 12438774]

Eylar EH, Madoff MA, Brody OV, Oncley JL. The Contribution of Sialic Acid to the Surface Charge of the Erythrocyte. J Biol Chem. 1962; 237:1992–2000. [PubMed: 13891108]

Fairhurst RM, Baruch DI, Brittain NJ, Ostera GR, Wallach JS, Hoang HL, Hayton K, Guindo A, Makobongo MO, Schwartz OM, Tounkara A, Doumbo OK, Diallo DA, Fujioka H, Ho M, Wellems TE. Abnormal display of PfEMP-1 on erythrocytes carrying haemoglobin C may protect against malaria. Nature. 2005; 435:1117–1121. [PubMed: 15973412]

Gardner MJ, Shallom SJ, Carlton JM, Salzberg SL, Nene V, Shoaibi A, Ciecko A, Lynn J, Rizzo M, Weaver B, Jarrahi B, Brenner M, Parvizi B, Tallon L, Moazzez A, Granger D, Fujii C, Hansen C, Pederson J, Feldblyum T, Peterson J, Suh B, Angiuoli S, Pertea M, Allen J, Selengut J, White O, Cummings LM, Smith HO, Adams MD, Venter JC, Carucci DJ, Hoffman SL, Fraser CM. Sequence of Plasmodium falciparum chromosomes 2, 10, 11 and 14. Nature. 2002; 419:531–534. [PubMed: 12368868]

Giribaldi G, Ulliers D, Mannu F, Arese P, Turrini F. Growth of Plasmodium falciparum induces stage-dependent haemichrome formation, oxidative aggregation of band 3, membrane deposition of complement and antibodies, and phagocytosis of parasitized erythrocytes. Br J Haematol. 2001; 113:492–499. [PubMed: 11380422]

Haldar K, Kamoun S, Hiller NL, Bhattacharje S, van Ooij C. Common infection strategies of pathogenic eukaryotes. Nat Rev Microbiol. 2006; 4:922–931. [PubMed: 17088934]

Haldar K, Mohandas N. Erythrocyte remodeling by malaria parasites. Curr Opin Hematol. 2007; 14:203–209. [PubMed: 17414208]

Hasted JB, Ritson DM, Collie CH. Dielectric properties of aqueous ionic solutions. J Chem Phys. 1948; 16:1–21.

Horrocks P, Pinches RA, Chakravorty SJ, Papakrivos J, Christodoulou Z, Kyes SA, Urban BC, Ferguson DJ, Newbold CI. PfEMP1 expression is reduced on the surface of knobless Plasmodium falciparum infected erythrocytes. J Cell Sci. 2005; 118:2507–2518. [PubMed: 15923663]

Jan KM, Chien S. Role of surface electric charge in red blood cell interactions. J Gen Physiol. 1973; 61:638–654. [PubMed: 4705641]

London E. How principles of domain formation in model membranes may explain ambiguities concerning lipid raft formation in cells. Biochim Biophys Acta. 2005; 1746:203–220. [PubMed: 16225940]

Maguire PA, Sherman IW. Phospholipid composition, cholesterol content and cholesterol exchange in Plasmodium falciparum-infected red cells. Mol Biochem Parasitol. 1990; 38:105–112. [PubMed: 2157152]

Maier AG, Cooke BM, Cowman AF, Tilley L. Malaria parasite proteins that remodel the host erythrocyte. Nat Rev Microbiol. 2009; 7:341–354. [PubMed: 19369950]

Murphy SC, Fernandez-Pol S, Chung PH, Prasanna Murthy SN, Milne SB, Salomao M, Brown HA, Lomasney JW, Mohandas N, Haldar K. Cytoplasmic remodeling of erythrocyte raft lipids during infection by the human malaria parasite Plasmodium falciparum. Blood. 2007; 110:2132–2139. [PubMed: 17526861]

Murphy SC, Samuel BU, Harrison T, Speicher KD, Speicher DW, Reid ME, Prohaska R, Low PS, Tanner MJ, Mohandas N, Haldar K. Erythrocyte detergent-resistant membrane proteins: their characterization and selective uptake during malarial infection. Blood. 2004; 103:1920–1928. [PubMed: 14592818]

Nagao E, Kaneko O, Dvorak JA. Plasmodium falciparum-infected erythrocytes: qualitative and quantitative analyses of parasite-induced knobs by atomic force microscopy. J Struct Biol. 2000; 130:34–44. [PubMed: 10806089]

Nagao E, Seydel KB, Dvorak JA. Detergent-resistant erythrocyte membrane rafts are modified by a Plasmodium falciparum infection. Exp Parasitol. 2002; 102:57–59. [PubMed: 12615167]

Overbeek, JTG. Electrokinetic Phenomena. Elsevier; Amsterdam: 1952. Electrochemistry of the doble layer.

Roggwiller E, Betoulle ME, Blisnick T, Braun Breton C. A role for erythrocyte band 3 degradation by the parasite gp76 serine protease in the formation of the parasitophorous vacuole during invasion of erythrocytes by Plasmodium falciparum. Mol Biochem Parasitol. 1996; 82:13–24. [PubMed: 8943147]

Tokumasu F, Dvorak J. Development and application of quantum dots for immunocytochemistry of human erythrocytes. J Microsc. 2003; 211:256–261. [PubMed: 12950474]

Tokumasu F, Fairhurst RM, Ostera GR, Brittain NJ, Hwang J, Wellems TE, Dvorak JA. Band 3 modifications in Plasmodium falciparum-infected AA and CC erythrocytes assayed by autocorrelation analysis using quantum dots. J Cell Sci. 2005; 118:1091–1098. [PubMed: 15731014]

Tokumasu F, Nardone GA, Ostera GR, Fairhurst RM, Beaudry SD, Hayakawa E, Dvorak JA. Altered membrane structure and surface potential in homozygous hemoglobin C erythrocytes. PLoS One. 2009; 4:e5828. [PubMed: 19503809]

Weiss L, Woodbridge RF. Some biophysical aspects of cell contacts. Fed Proc. 1967; 26:88–94. [PubMed: 6018929]

Highlights

P. falciparum infection reduced parasitized RBC zeta potential (Z.P.).

The reduction was independent of sialic acid.

The reduction of Z.P. increased cytoadherence of parasitized RBC.

Presence of ‘knobs’ changes the distributions of zeta potential.

Influence of trypsin-treatment was tested for both knobby and knobless parasites.

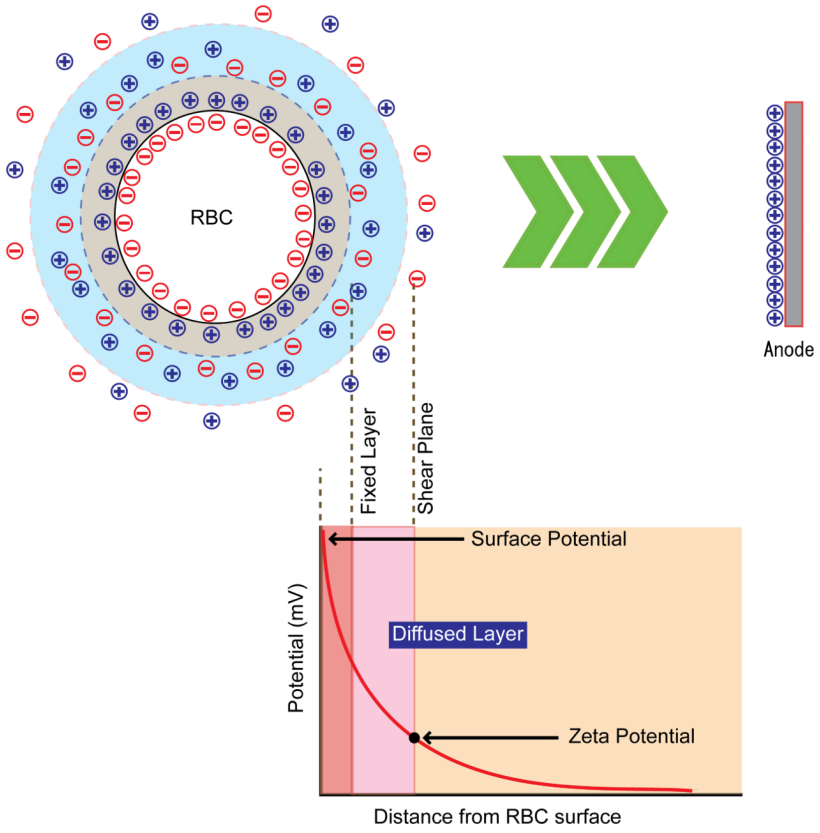

Figure 1.
Basic concept of zeta potential (ZP). Negatively-charged red blood cells migrate toward the positive electrode upon the application of voltage between positive and negative electrodes.

ZP is defined as $\zeta = A \cdot \frac{4\pi\eta}{\varepsilon} \cdot U$ and $U = \frac{\nu}{V/L}$, where A is a constant, ζ is the zeta potential, η is the viscosity of solution, ε is the dielectric constant, and U is the electrophoretic mobility, ν is the speed of particle, V is the applied voltage, and L is the distance of electrode (Overbeek, 1952, Weiss and Woodbridge, 1967). Dielectric constant and viscosity of the buffer is approximated as those of water.

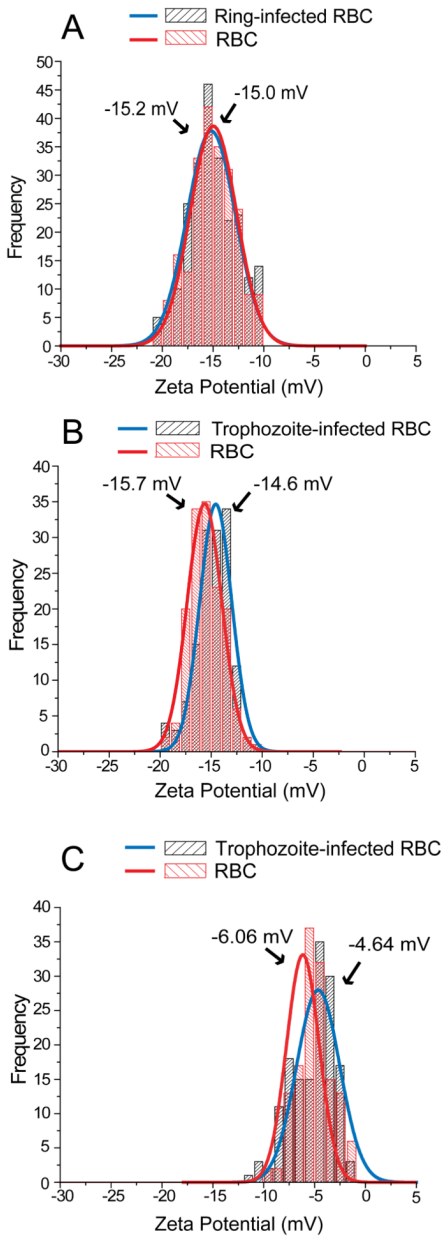

Figure 2.

Zeta potential (ZP) of red blood cell (RBC) samples. (A) ZP of *P. falciparum* ring-infected RBCs. (B) ZP of *P. falciparum* trophozoite-infected RBCs. (C) ZP of *P. falciparum* trophozoite-infected RBCs treated with neuraminidase. Curves represent Gaussian fitting of the data. Small differences in the peak value and distribution of ZP between RBC samples from different donors may have resulted from differences in the age-distribution of their RBCs.

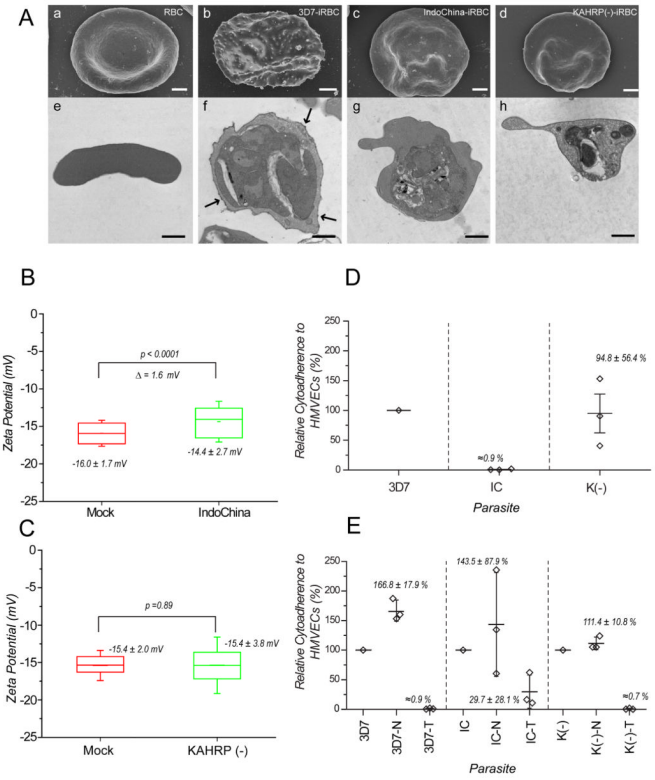

Figure 3.

Influence of knobs on zeta potential (ZP) and cytoadherence. (A) Electron micrographs of knobby and knobless *P. falciparum* trophozoite-infected red blood cells (iRBCs). Panels a–d: scanning electron microscopic images. Panels e–h: transmission electron microscopic images. Bar represents 1 μm. (B, C) ZP values of iRBCs containing Indochina and KAHRP(−) 3D7 parasites, respectively, compared to mock-cultured RBC controls. (D) Relative cytoadherence of iRBCs containing knob-forming (3D7) and knobless (Indochina, KAHRP(−) 3D7) parasite clones. An average of 1.2 3D7 iRBCs were bound per MVEC. (E) Effects of neuraminidase and trypsin treatments on cytoadherence of iRBCs containing 3D7, Indochina, or KAHRP(−) 3D7 *P. falciparum* clones. Cytodherence levels of untreated iRBCs were set at 100%.

Table

Samples	Z.P. (mV)	r^2	$p^{\#}$	*n*
RBC	−15.0 ± 0.10	0.97	0.93	222
Ring-infected RBC *	−15.2 ± 0.13	0.95		234
RBC	−15.7 ± 0.06	0.98	<0.001	147
Trophozoite-infected RBC **	−14.6 ± 0.07	0.97		140
Neuraminidase-treated RBC	−6.06 ± 0.14	0.93	<0.001	137
Neuraminidase-treated iRBC *	−4.64 ± 0.35	0.75		150

Peak Z.P ± (fitting error) is shown.

* Parasitemia ≈10%,

** Parasitemia >80%,

Two-sample independent t-test. *n* represents the number of cells measured.